

Thermoelectric power of the $(\text{Eu,Ce})_4(\text{Ba,Eu})_4\text{Cu}_6\text{O}_y$ phase and the T^* phase: Comparison between superconducting and nonsuperconducting compounds

S. Ikegawa,* T. Wada, T. Yamashita, A. Ichinose, K. Matsuura, K. Kubo, H. Yamauchi, and S. Tanaka
Superconductivity Research Laboratory, International Superconductivity Technology Center,

10-13 Shinonome 1-chome, Koto-ku, Tokyo 135, Japan

(Received 30 November 1990; revised manuscript received 23 January 1991)

The Seebeck coefficient (\mathcal{S}) and Hall coefficient (R_H) are measured in the temperature range 20–310 K for $(L_{2/3}\text{Ce}_{1/3})_4(\text{La}_{1/3}\text{Ba}_{1/3}\text{Sr}_{1/3})_4\text{Cu}_6\text{O}_y$ (4:4:6 phase) with $L=\text{Eu}$ (superconducting) and $L=\text{Y}$ (nonsuperconducting), and $\text{Nd}_{1.4}\text{Ce}_{0.2}\text{Sr}_{0.4}\text{Cu}_{1-x}\text{Zn}_x\text{O}_{4-\delta}$ (T^* phase) with $x=0$ (superconducting) and $x=0.015$ (nonsuperconducting). In both the 4:4:6 phase and the T^* phase, the R_H of the nonsuperconducting compound is nearly the same as that of the superconducting compound, at temperatures higher than 150 K, but \mathcal{S} of the nonsuperconducting compound is larger than that of the superconducting compound throughout the measured temperature range. This suggests that the contribution from carrier scattering to \mathcal{S} is different in the nonsuperconducting and superconducting compounds. The temperature dependence of \mathcal{S} for these compounds is compared with a theoretical prediction for the resonating-valence-bond state.

The normal-state electrical-transport properties of various cuprates have been studied to elucidate the underlying mechanisms of high-temperature superconductivity.^{1,2} The Seebeck effect is one of the transport properties complementary to the Hall effect and electrical conductivity. For most of the superconducting cuprates, around room temperature the magnitude of the Seebeck coefficient (\mathcal{S}) for sintered samples decreases with increasing temperature.² This behavior of \mathcal{S} is contrary to that known for uncorrelated electrons in conventional metals.

For $(L_{2/3}\text{Ce}_{1/3})_4(\text{La}_{1/3}\text{Ba}_{1/3}\text{Sr}_{1/3})_4\text{Cu}_6\text{O}_y$ where L is a rare-earth element and located in the fluorite-type block in the crystal structure [that is it has a $(\text{Eu,Ce})_4(\text{Ba,Eu})_4\text{Cu}_6\text{O}_y$ -type phase³ or a 4:4:6 phase], Wada *et al.*⁴ reported that the magnitude of T_c strongly depended on the radius of the L^{3+} ion. This contrasts to the case of $\text{LBa}_2\text{Cu}_3\text{O}_7$ (1:2:3 phase) where the magnitude of T_c depends little on the radius of the L^{3+} ion. The samples of 4:4:6-phase compounds with $L=\text{Eu}$, Dy, Y, and Ho had nearly identical oxygen contents⁴ and Hall coefficients when the temperature was between room temperature and 150 K.⁵ Therefore, T_c of $(L_{2/3}\text{Ce}_{1/3})_4(\text{La}_{1/3}\text{Ba}_{1/3}\text{Sr}_{1/3})_4\text{Cu}_6\text{O}_y$ must be controlled by some unknown factors (other than the hole concentration) which may be related to the radius of the L^{3+} ion. In this work, we measured the Seebeck coefficients for ceramic samples of the 4:4:6 phase and the T^* phase to investigate the unknown factors.

Two sets of samples were prepared. Each of the sets consisted of two samples having nearly the same carrier concentration, one being superconducting ($T_c > 20$ K) and the other nonsuperconducting ($T_c < 2$ K). The superconducting transition temperature T_c was defined by the onset of the diamagnetic signal in dc magnetic susceptibility. The first set consisted of $(L_{2/3}\text{Ce}_{1/3})_4(\text{La}_{1/3}\text{Ba}_{1/3}\text{Sr}_{1/3})_4\text{Cu}_6\text{O}_y$ with $L=\text{Eu}$ (Eu 4:4:6) and $L=\text{Y}$ (Y 4:4:6). The samples were prepared by the same procedure as that given in Refs. 4 and 5. T_c for Eu 4:4:6 was 28.5 K. For Y 4:4:6 no superconducting transition was observed down to

2 K. This corresponds to the fact that T_c decreases as the size of the L^{3+} ion decreases.⁴

The samples of the second set were $\text{Nd}_{1.4}\text{Ce}_{0.2}\text{Sr}_{0.4}\text{Cu}_{1-x}\text{Zn}_x\text{O}_{4-\delta}$ with $x=0$ ($T^*\text{S}$) and $x=0.015$ ($T^*\text{N}$), which were prepared⁶ by a standard solid-state reaction method. Both samples were sintered at 1150°C for 10 h followed by annealing at 500°C for 10 h in O_2 -gas flow and confirmed to be of single phase of the T^* -type by x-ray powder diffraction. As the Zn content x increased, T_c decreased monotonically.⁶ The T_c 's for the samples with $x=0$ and 0.015 were 23.1 K and less than 2 K, respectively. For comparison, parallel measurements were made for a sintered sample⁶ of $\text{La}_{1.85}\text{Sr}_{0.15}\text{CuO}_{4-\delta}$ (T phase: $T_c=38.3$ K).

The Seebeck coefficients were measured by a dc differential method at temperatures between 20 and 310 K. The temperature and temperature gradient across the sample were measured using a calibrated Si-diode sensor and two pairs of copper-Constantan thermocouples, respectively. The Cu wires of 50- μm diameter were used as the reference metal. The sample dimension was $7 \times 2.5 \times 1$ mm³. The Hall-effect and resistivity measurements were simultaneously made under the same conditions as those employed in Ref. 5.

The Seebeck coefficient \mathcal{S} for $\text{La}_{1.85}\text{Sr}_{0.15}\text{CuO}_{4-\delta}$ is plotted in Fig. 1 with open circles. The \mathcal{S} -vs- T curve has a maximum around 90 K, as previously reported.^{2,7} Figure 1 also includes the data for the temperature dependence of \mathcal{S} and resistivity (ρ) for the 4:4:6 samples. The \mathcal{S} -vs- T curve for Eu 4:4:6 (crosses in Fig. 1) has a peak (at T_q) around 170 K and is nearly identical with that for $\text{La}_{1.85}\text{Sr}_{0.15}\text{CuO}_{4-\delta}$ at temperatures above 200 K. Throughout the measured temperature range, \mathcal{S} for Y 4:4:6 (solid triangles in Fig. 1) is larger than that for Eu 4:4:6. T_q for Y 4:4:6 is 190 K, which is slightly higher than that for Eu 4:4:6. The resistivity of Y 4:4:6 is larger than that for Eu 4:4:6, especially at temperatures below 100 K. Each of the ρ -vs- T curves possesses a minimum between 120–130 K. The Hall coefficients (R_H) of the

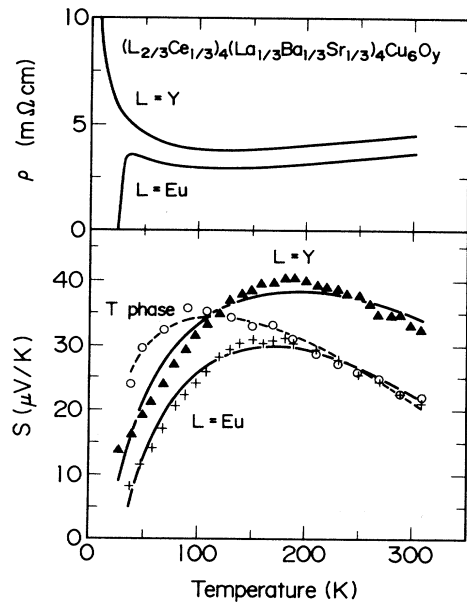


FIG. 1. Temperature dependence of Seebeck coefficients and resistivity for $(L_{2/3}\text{Ce}_{1/3})_4(\text{La}_{1/3}\text{Ba}_{1/3}\text{Sr}_{1/3})_4\text{Cu}_6\text{O}_y$ with $L=\text{Eu}$ (Eu 4:4:6, $T_c=28.5$ K) and $L=\text{Y}$ (Y 4:4:6, $T_c<2$ K). Seebeck coefficients for $\text{La}_{1.85}\text{Sr}_{0.15}\text{CuO}_{4-\delta}$ (T phase) are also shown by open circles. The curves in the lower portion show fits to Eq. (1).

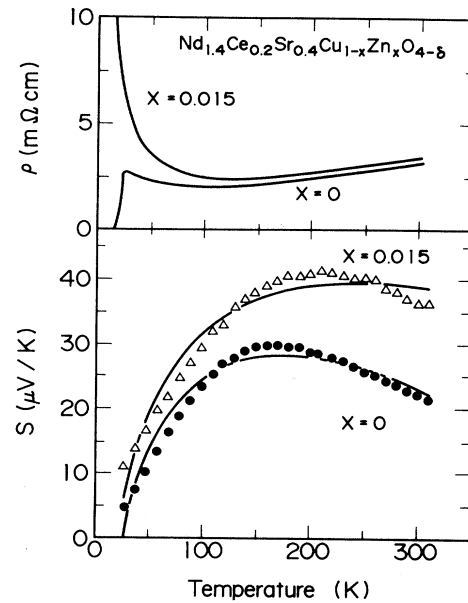


FIG. 2. Temperature dependence of Seebeck coefficients and resistivity for $\text{Nd}_{1.4}\text{Ce}_{0.2}\text{Sr}_{0.4}\text{Cu}_{1-x}\text{Zn}_x\text{O}_{4-\delta}$ with $x=0$ ($T^*\text{S}$, $T_c=23.1$ K) and $x=0.015$ ($T^*\text{N}$, $T_c<2$ K). The curves in the lower portion show fits to Eq. (1).

two samples were identical, within an uncertainty of $\pm 4\%$, at temperatures higher than 150 K (see Fig. 2 of Ref. 5). R_H of these samples exhibited a broad peak with respect to temperature located around 110–130 K.⁵

Figure 2 shows the temperature dependence of \mathcal{S} and ρ for the T^* samples. The \mathcal{S} -vs- T curve for $T^*\text{S}$ (solid circles in Fig. 2) shows a maximum at $T_q=160$ K. When the Cu sites are substituted by Zn, the magnitude of \mathcal{S} is raised throughout the measured temperature range, and T_q shifts from 160 K to 210 K. At the same time, the magnitude of ρ is increased especially at temperatures lower than 150 K. Each of the ρ -vs- T curves has a minimum at 110–130 K. The Hall coefficients for the $T^*\text{N}$ at temperatures higher than 150 K are nearly the same as those of the $T^*\text{S}$ as shown in Fig. 3. The temperature dependence of R_H for each of these samples exhibits a peak in the temperature range of 130–150 K, and, at temperatures lower than the peak temperature, the slope of the R_H -vs- T curves decreases with decreasing T_c , as previously observed for the 4:4:6 samples.⁵

The \mathcal{S} -vs- T curves for the 4:4:6 (Fig. 1) and T^* phases (Fig. 2) are slightly different from that for $\text{La}_{1.85}\text{Sr}_{0.15}\text{CuO}_{4-\delta}$ (Fig. 1). The superconducting samples of both the 4:4:6 and T^* phases, i.e., Eu 4:4:6 and $T^*\text{S}$, show nearly identical \mathcal{S} -vs- T curves. For each of the two phases, the difference in \mathcal{S} of the nonsuperconducting and superconducting samples ($\Delta\mathcal{S}$) is plotted with respect to temperature in Fig. 4. The temperature dependence of $\Delta\mathcal{S}$ for the 4:4:6 samples is similar to that for the T^* samples. At low temperatures (below 150 K for the 4:4:6 phase and below 130 K for the T^* phase), $\Delta\mathcal{S}$ is independent of temperature. At high temperatures, $\Delta\mathcal{S}$ increases

with increasing temperature, although the data for temperatures above 260 K are rather scattered probably because of poor temperature control. Thus, the differences in \mathcal{S} , R_H , and ρ of the nonsuperconducting and superconducting samples seem to be qualitatively different in the high- and low-temperature ranges, being separated around 110–150 K. The experimental results for both the 4:4:6 and T^* samples are summarized as follows: (1) In the high-temperature range—higher than 150 K— R_H of the nonsuperconducting compound is nearly identical with that of the superconducting compound, and also the ρ 's of

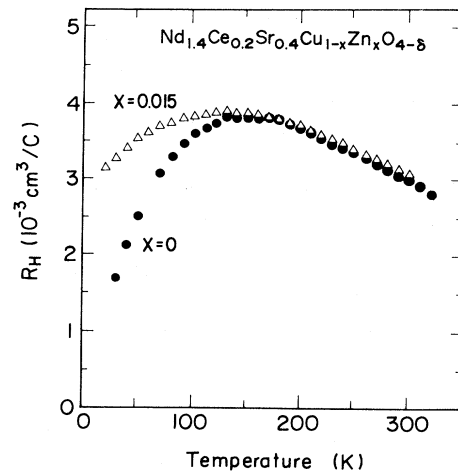


FIG. 3. Temperature dependence of Hall coefficients for $\text{Nd}_{1.4}\text{Ce}_{0.2}\text{Sr}_{0.4}\text{Cu}_{1-x}\text{Zn}_x\text{O}_{4-\delta}$ with $x=0$ ($T^*\text{S}$) and $x=0.015$ ($T^*\text{N}$).

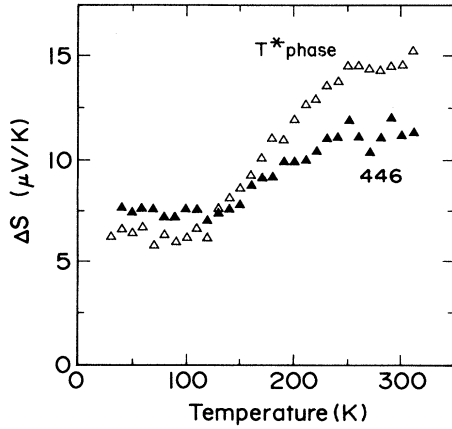


FIG. 4. Difference in Seebeck coefficients (ΔS) between the nonsuperconducting and superconducting compounds with respect to temperature. The solid triangles and open triangles indicate the case of the 4:4:6 phase and the case of Zn doping in the T^* phase, respectively.

the two compounds are not very different; (2) in the same temperature range, however, \mathcal{S} of the nonsuperconducting compound is larger than that of the superconducting compound; (3) in the low-temperature range lower than 150 K, the nonsuperconducting compound has larger \mathcal{S} , R_H , and ρ than those of the superconducting compound.

It was reported⁷ for $(\text{La}, \text{Ba})_2\text{CuO}_4$ and $\text{YBa}_2\text{Cu}_3\text{O}_{7-\delta}$ that, when the density of doped holes decreased, both \mathcal{S} and R_H increased in the temperature range between T_c and 300 K. In the present work, result (2) may not be caused by a difference in the hole density but by a difference in the carrier-scattering contribution, because of result (1). On the other hand, in the low-temperature range, result (3) implies that the mobile-carrier concentrations of the nonsuperconducting and superconducting compounds are different.⁵ Nonetheless, the relation between the high- and low-temperature transport properties is not clear.

So far it has been demonstrated that the difference in the transport properties between Y 4:4:6 and Eu 4:4:6 appears to be parallel to that between $T^*\text{N}$ and $T^*\text{S}$, in spite of the fact that the nature of Eu(Y) atomic site in the 4:4:6 phase is different from that of Cu(Zn) atomic site in the T^* phase. Therefore, the dependence of T_c on the size of the L^{3+} ion in the 4:4:6 phase and the decrease in T_c by Zn doping in the T^* phase are suspected to have the same origin. The substitution of Zn for Cu in the T^* phase is expected to cause a deterioration in the antiferromagnetic correlations between Cu^{2+} spins⁶ and a disorder (in the potential energy) in the CuO_2 planes. These effects may bring about additional carrier scattering and/or a change in the energy dependence of the carrier mean free path, and consequently an increase in \mathcal{S} . In the 4:4:6 phase, a similar disorder may be caused in the CuO_2 planes by the change in the radius of the L^{3+} ion. Such a disorder may be induced by oxygen defects in the fluorite-type block in the crystal, and the mismatch in the lattice dimension between the CuO_2 plane and the underlying fluorite-type block.

TABLE I. Fitted parameters, F , G , and H for Eq. (1). (Sample names are defined in the text.)

Sample	F	G (K)	H (K)
Eu 4:4:6	0.408 ± 0.011	352 ± 16	414 ± 11
Y 4:4:6	0.333 ± 0.017	426 ± 43	575 ± 35
$T^*\text{S}$	0.339 ± 0.017	529 ± 58	515 ± 28
$T^*\text{N}$	0.307 ± 0.018	596 ± 79	798 ± 70
T phase	0.2422 ± 0.0013	581 ± 7	480.4 ± 1.7

Recently, using a gauge-field theory for a uniform resonating-valence-band (RVB) state, Nagaosa and Lee⁸ proposed that, for the superconducting cuprates, $\mathcal{S} = \mathcal{S}_F + \mathcal{S}_B$ (NL model), where \mathcal{S}_F and \mathcal{S}_B were estimated—using the Fermi statistics and Maxwellian statistics, respectively—to be $-(k_B/e)k_B T/E_F$ and $(k_B/e)[1 - \ln(2\pi p_{\text{sh}}/mk_B T)]$. The p_{sh} denotes concentration of holes on CuO_2 sheets per $[\text{Cu-O}]$. In order to fit the present experimental data to this equation, m and E_F were regarded as fitting parameters. However, thus-fitted curves were not in reasonable agreement with the experimental data. An additional parameter F may be introduced as follows:

$$\mathcal{S}(T) = (k_B/e)[1 - F \ln(2\pi p_{\text{sh}} G/T) - T/H], \quad (1)$$

where F , G , and H are fitting parameters. Assuming $p_{\text{sh}} = 0.14$ for all the samples and using a least-squares method, these three parameters were determined for each sample, as listed in Table I. In the NL model,⁸ the values for parameters G ($\sim m^{-1}$) and H ($\sim E_F$) are expected to be of the order of the exchange energy $J \sim 1000$ K. The values for G and H given in Table I are roughly of the same order as those anticipated by the NL model. The solid and dashed curves in the lower portion of Figs. 1 and 2 are the fitted curves using Eq. (1). These fitted curves, especially for Eu 4:4:6, $T^*\text{S}$, and T samples, are in good agreement with the experimental curves. Therefore, if the temperature dependence of \mathcal{S} is given by the relation: $\mathcal{S} = \mathcal{S}_F + \mathcal{S}_B$, the logarithmic term in \mathcal{S}_B is required to be modified by parameter F . This suggests that the chemical potential of the boson system is smaller (by a factor $F \sim 0.3$) than that of the Maxwell distribution in the two-dimensional system employed in the NL model. Equation (1) can explain the decrease in \mathcal{S} with increasing temperature at room temperature and the maximum of \mathcal{S} at 100–250 K that have been often observed for superconducting cuprates.² It should be noted, however, that the present \mathcal{S} -vs- T curves at temperatures below 100 K show a linear behavior rather than the logarithmic behavior of Eq. (1). Alternative explanations for the discrepancy between the experimental results and the NL model can be made based on certain carrier-dragging effects by phonons, spins, and/or gauge field (photons).

In summary, the Seebeck coefficients for $(L_{2/3}\text{Ce}_{1/3})_4\text{-(La}_{1/3}\text{Ba}_{1/3}\text{Sr}_{1/3})_4\text{Cu}_6\text{O}_y$ ($L = \text{Eu}$ and Y) and $\text{Nd}_{1.4}\text{-Ce}_{0.2}\text{Sr}_{0.4}\text{Cu}_{1-x}\text{Zn}_x\text{O}_{4-\delta}$ ($x = 0$ and 0.015) were positive and had maxima around 160–210 K. For each of the 4:4:6 phase and the T^* phase in the high-temperature range ($T > 150$ K), R_H of the nonsuperconducting compound (i.e., Y 4:4:6 or $T^*\text{S}$) was nearly the same as that of the superconducting compound, but \mathcal{S} of the nonsuper-

conducting compound was larger than that of the superconducting compound. This suggests that the contribution from carrier scattering to \mathcal{S} is different between the nonsuperconducting and superconducting compounds. In the low-temperature range ($T < 150$ K), the nonsuperconducting compound had larger values not only for \mathcal{S} but also for R_H and ρ than those of the superconducting com-

pound. Further studies are required to determine the relation between the high-temperature ($T > 150$ K) and low-temperature ($T < 150$ K) transport properties.

We would like to thank Dr. N. Nagaosa, Dr. S. Uchida, and Dr. H. Takagi of the University of Tokyo for their helpful discussions.

*Present address: Advanced Research Laboratory, Toshiba Research & Development Center, 1, Komukai Toshiba-cho, Saiwai-ku, Kawasaki, 210, Japan.

¹For a review, see N. P. Ong, in *Physical Properties of High-Temperature Superconductors II*, edited by D. M. Ginsberg (World Scientific, Singapore, 1990), p. 468.

²For a review, see A. B. Kaiser and C. Uher, in *Studies of High Temperature Superconductors*, edited by A. V. Narlikar (Nova Science, New York, 1990), Vol. 7.

³H. Sawa, K. Obara, J. Akimitsu, Y. Matsui, and S. Horiuchi, *J. Phys. Soc. Jpn.* **58**, 2252 (1989).

⁴T. Wada, A. Ichinose, Y. Yaegashi, H. Yamauchi, and S. Ta-

naka, *Jpn. J. Appl. Phys.* **29**, L266 (1990).

⁵S. Ikegawa, T. Wada, A. Ichinose, T. Yamashita, T. Sakurai, Y. Yaegashi, T. Kaneko, M. Kosuge, H. Yamauchi, and S. Tanaka, *Phys. Rev. B* **41**, 11 673 (1990).

⁶S. Ikegawa, T. Yamashita, T. Sakurai, R. Itti, H. Yamauchi, and S. Tanaka, *Phys. Rev. B* **43**, 2885 (1991).

⁷H. Ishii, H. Sato, N. Kanazawa, H. Takagi, S. Uchida, K. Kitazawa, K. Kishio, K. Fueki, and S. Tanaka, *Physica* **148B**, 419 (1987).

⁸Naoto Nagaosa and Patrick A. Lee, *Phys. Rev. Lett.* **64**, 2450 (1990).